A Comparison of Biogeochemical Argo Sensors, Remote Sensing Systems, and Shipborne Field Fluorometers to Measure Chlorophyll *a* Concentrations in the Pacific Ocean off the Northern Coast of New Zealand

Amy Phung
Olin College of Engineering
Needham MA, USA

***Abstract*—Accurately measuring chlorophyll *a* concentrations within the world's oceans is an important part of building our understanding of its underlying processes and the human impact on it, and developing tools to do this is an area of active study. Some methods used today to collect this data include in-situ fluorometers on board automated Biogeochemical Argo floats, flow-through fluorometers on board oceangoing vessels, and ocean color algorithms applied to remote sensing data. While shipborne field fluorometers are the most accurate of the three since they can be recalibrated before and after each expedition, they are limited in spatial and temporal coverage due to their dependence on expensive oceanographic research cruises. The Biogeochemical floats help to increase the coverage of fluorometer data by automating the data collection, but are known to suffer from sensor drift over time since their fluorometers cannot be serviced and calibrated regularly. Remote sensing data has by far the greatest spatial and temporal coverage of the three methods, but is known to be significantly less accurate in certain regions and is limited to surface measurements. This study compares these three measurement methods by analyzing data collected by a 10AU Field and Laboratory Fluorometer connected to a flow-through system, data from a Biogeochemical Argo float, and satellite data from the VIIRS-SNPP dataset in the same region. The results of comparisons between each of these collection methods are presented.**

***Index Terms*—Chlorophyll *a* measurement, remote sensing, Biogeochemical Argo, field fluorometers, VIIRS-SNPP, sensor comparison**

I. Introduction

Accurate chlorophyll *a* concentration measurements are critical for studying the global carbon, nitrogen, and oxygen cycles since chlorophyll concentrations are indicative of phytoplankton abundance and consequently ocean productivity. While these cycles have been important since the beginnings of life on Earth, there's been a surge of interest in studying these processes due to ocean acidification and climate change directly attributed to human activities. Because ocean circulation is a central component to these critical processes, it is useful to collect not only surface-level data, but also to measure chlorophyll *a* levels at varying depths within the water column (Behrenfeld and Falkowski, 1997). [1] The ocean plays a major role in providing us with the air we breathe, the climate we live in, and the food we consume, so it is imperative that we develop the necessary tools to understand our impact on it.

Currently, large-scale chlorophyll *a* measurements are collected via remote sensing with ocean color algorithms applied to satellite imagery, which is useful for obtaining global data at regular time intervals (Carder et al., 2004). [2] This data has numerous applications, and has been extensively used to monitor and study natural ocean processes such as primary production, ocean circulation, and harmful algal blooms. On the human impacts front, this data's uses range from documenting the status of coastal water quality to mitigating effects from major oil spills (Hu and Campbell). [3] Our heavy reliance on these ocean color algorithms emphasizes the importance that this data is verified by in-situ measurements, (Smith et al., 1981) [4] particularly since the accuracy of chlorophyll *a* measurements taken by color satellites has been documented to vary by region and concentration (Hu et al., 2012). [5] It's worth noting that this technology suffers from resolution limitations, is hindered by cloud cover, and doesn't capture information at depth since it can only capture information within the ocean's euphotic zone (Kahru, 2016; Lee et al., 2007), [6], [7] which highlights the need for alternative measurement methods that can overcome these limitations.

While in-situ measurements are a precise way to measure chlorophyll concentrations and are important for validating ocean color algorithms, these discrete measurements only provide information for infinitesimally small points over the ocean's surfaces (Behrenfeld and Falkowski, 1997). [1] Taking these measurements requires a team of dedicated scientists, a professional ship's crew, and a properly equipped oceangoing vessel to reach remote study sites, causing them to be sparse, expensive to acquire, and often inconsistent since sampling locations and timing are dependent on current scientific interests (Glenn et al., 2000). [8]

An ongoing project to automate the collection of in-situ chlorophyll *a* data at varying depths in the water column is the Biogeochemical Argo float project, where a network of free-drifting floats are used to take measurements of temperature, salinity, pH, oxygen, nitrate, chlorophyll, suspended particles, and downwelling irradiance at depths up to 2000 meters. A sufficiently large network of floats measuring these additional variables would vastly expand the potential for global ocean prediction systems and the management of living marine resources (http://www.argo.ucsd.edu, Bittig et al., 2019). [9]

While the development of Biogeochemical Argo floats is a promising start towards chlorophyll *a* measurements at depth, it is not without limitations. The floats are equipped

with fluorometers to measure chlorophyll *a* concentrations, but since the floats are free-floating, regular retrieval for re-calibration of its sensors is impractical. Like other long-term sensor deployments (e.g. moorings or seagliders), the float's calibration can be affected by vibrations during shipping, physical damage to the sensors, or bio-fouling. (Earp et al., 2011) [10] As a result, these floats are known to have issues with sensor drift over time. (Chang and Gould, 2006). [11]

Previous studies directly compared in-situ chlorophyll measurements with satellite-derived chlorophyll data and found systematic error trends of chlorophyll measurements between different oceans (Szeto et al. 2011). [12] In the Southern Ocean and other high-latitude waters, Guinet et al. [13] found that satellite chlorophyll measurements were consistently lower than in-situ measurements in the same region. Other studies found that in the Pacific Ocean in mid to high-latitude waters, chlorophyll concentrations measured by remote sensing systematically exceeded the values measured by laser fluorometers (Bukin et al., 2001). [14] Several previous studies highlighted the need for regional ocean color algorithms to minimize this discrepancy and improve accuracy (e.g. Johnson et al., 2017; Kahru and Mitchell, 2010; Szeto et al., 2011) [6], [12], [15] For the Biogeochemical Argo floats, a previous study suggests satellite ocean color measurements of chlorophyll can potentially provide some measure of real time validation and sensor drift (Roesler et al., 2017). [16]

The objectives of this paper are to 1) measure the discrepancy between chlorophyll *a* data obtained by a shipborne flow-through fluorometer, via fluorometers equipped on Biogeochemical Argo floats, and via ocean color algorithms applied to remote sensing data in the Pacific off the coast of New Zealand 2) document the extent of the discrepancy in this particular region and 3) find trends in the discrepancy to quantify the extent of the sensor drift of Biogeochemical floats in the area.

II. Methods

A. Flow-Through Data: Collection

The flow-through data used in this study was collected by SEA Semester students on board the SSV *Robert C. Seamans* along a cruise track off the northern coast of New Zealand from February 18th to March 12th, 2020. Chlorophyll *a* data was collected on-board through two fluorometers – a 10AU Field and Laboratory Fluorometer collecting continuous surface flow-through fluorescence data, and a Sea Point in-vivo chlorophyll *a* fluorometer equipped on a hydrocast carousel to collect data at depth. This study will primarily focus on the data collected from the flow-through, but will rely on the hydrocast data for calibration. To increase the sample size for the flow-through measurements, the raw fluorescence data was first pre-processed with a 1-minute binned average before any further analysis was conducted.

B. Flow-Through Data: Hydrocast Calibration

In order for the data to be useful as a basis for comparison to other data sources, it needed to be properly calibrated and converted to standard units. In order to achieve this, 81 water samples were collected across 29 stations at varying depths with Niskin bottles and were vacuum filtered for chlorophyll in dim light. This process produced a chlorophyll *a* measurement in units of $\mu g/L$ for these samples. A linear Total Least Squares (TLS) model [1] [17] was then fit to these data points using Python to quantify the relationship between the raw output voltage of the fluorometer and the actual chlorophyll *a* levels in $\mu g/L$. The results from this process can be viewed in Figure 1.

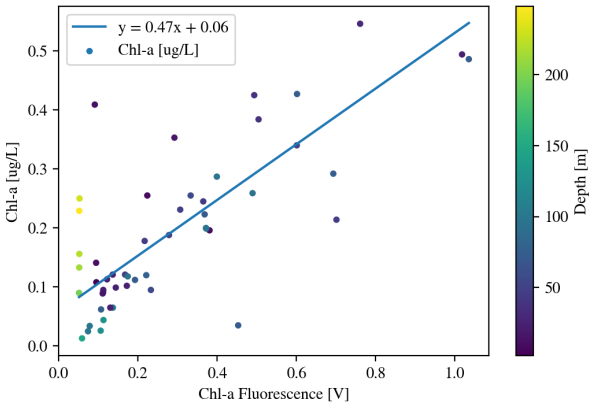

Fig. 1. Best-fit TLS model relating raw output voltage of the hydrocast fluorometer to measured chlorophyll *a* values with sample depth information illustrated

This model was then applied to the rest of the hydrocast fluorometer data to convert all of the raw measurements to estimated chlorophyll *a* values in $\mu g/L$.

C. Flow-Through Data: Fluorometer Calibration

Before calibration, the flow-through dataset needed to be filtered in order to achieve optimal results. For starters, data collected during the ship's port stops was removed. Since the flow-through system is not designed to collect data while the ship is stationary, the integrity of the data collected during these time periods cannot be ensured. Points which deviated more than three standard deviations ($> 3\sigma$) from the mean were considered outliers and were also removed from the set. To filter out remaining variability, a 31-point median filter was applied. [2] The results of this filtering can be viewed in Figure 2.

Before moving forward with the analysis, it's worth taking a closer look at the data to evaluate whether or not the proposed

[1] A TLS model, synonymous with Orthogonal Distance Regression (ODR) for linear models, was chosen over an Ordinary Least Squares (OLS) model since it better accounts for measurement variance in both the 'predictor' and 'estimator' variables opposed to just the 'predictor'

[2] A median filter was chosen since the variability was relatively infrequent but resulted in points that significantly differed from the general trend. A moving average filter would have required averaging more points in order to achieve the same efficacy, which would've decreased the resolution of the data. 31 points were used in the median filter because the ship generally traveled at a speed of around 5 knots, which meant that 31 points would be looking at around 2.5 nautical miles' worth of data. Since the overall objective is to compare this data to the VIIRS-SNPP dataset with a resolution of 4 kilometers (approx. 2.1 nautical miles), 31 was a good number to choose to make the resolution of both datasets similar.

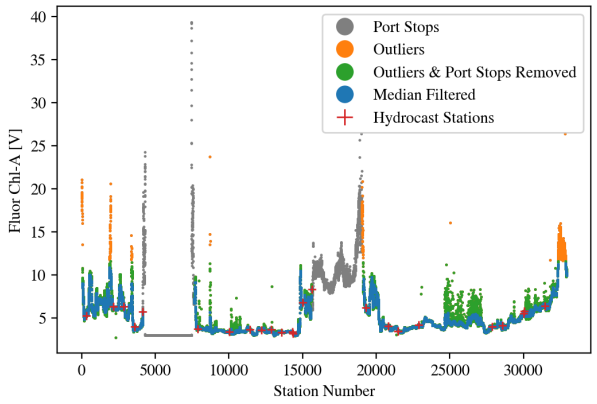

Fig. 2. Graph displaying fluorescence data at various stages of pre-processing. Data collected during port stops and outliers (points which deviated $> 3\sigma$ from the mean) were removed from the dataset. The points left over after these filters were applied are highlighted in green. A median filter with a window size of 31 was applied to the points left over to filter out variability. Points with corresponding hydrocast data that were used for calibration are highlighted in red.

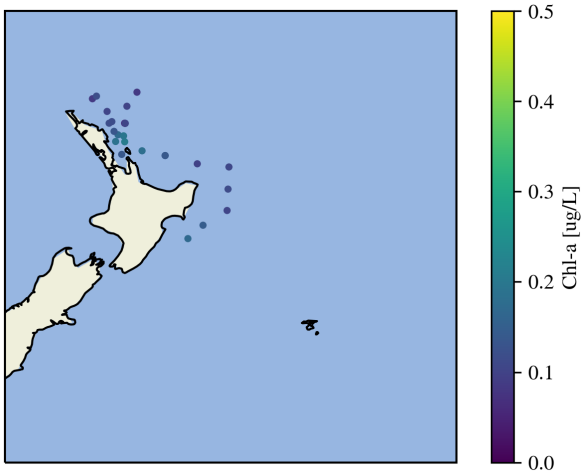

Fig. 3. Locations and calibrated values of surface hydrocast data points used to calibrate flow-through dataset displayed on map

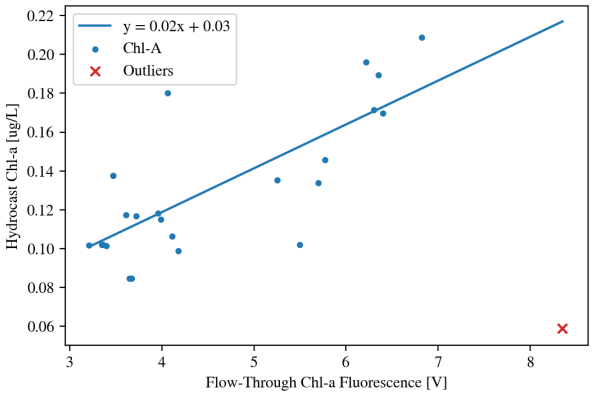

Fig. 4. Flow-through fluorescence values compared with computed chlorophyll *a* values from hydrocast surface measurements. A best-fit line computed with RANSAC describes the relationship between the two sensors after outlier removal

filtering and data pre-processing methods are acceptable. The original recorded data is a 1-minute binned average, which translates to a seawater sample size of between 50 to 600 mL per data point (based on the recommended flow rate range for the Turner Designs fluorometer). Considering the small sample size in conjunction with spatial heterogeneity of seawater samples (e.g. an algae patch caused by shifting oceanic fronts), transient periods of high readings when passing through these regions are expected, particularly since tens of thousands of 1-minute samples will be collected over the course of the cruise. This expected behavior is consistent with the occasional sharp voltage spikes observed in the original data (illustrated by the green and orange points in Figure 2). If left in the dataset, these spikes would add an unrepresentative skew towards higher chlorophyll readings since these patches are not necessarily indicative of general trends in the area. Based on this examination, we can prudently move forward with the analysis using the filtered data.

Unlike the calibration process used for the hydrocast data, calibrating the flow-through by directly comparing the filtered samples with the flow-through fluorescence data would be unreasonable due to the fact that most of the water samples filtered for chlorophyll *a* were collected at depths significantly lower than what the flow-through would observe. In lieu of this, the flow-through fluorescence data was calibrated by comparing surface hydrocast data after applying the model from Figure 1 with the voltage of the filtered flow-through fluorometer during the time closest to when the surface data was collected. Locations and calibrated values of the surface hydrocast data is displayed in Figure 3. A comparison between these data points can be viewed in Figure 4.

The RANSAC algorithm implemented by Pedregosa et al. [18] was used to identify outliers and fit a linear model to the data in Figure 4. This process classified one point as an outlier, which came from the hydrocast station right before the second port stop. Considering that the hydrocast fluorometer's sensing volume is a mere 0.34 mL and the flow-through sample size is between 50 to 600 mL as previously mentioned, it is plausible that one or both of these measurements were based on a seawater sample not representative of the area. Therefore, we chose to accept the best fit line computed by RANSAC and omit the outlier from the calibration data set. The computed model was then applied to the rest of the flow-through fluorescence data to compute chlorophyll *a* values based on the output voltage. The results of these computations can be viewed in context of each point's geographic location in Figure 5.

D. Biogeochemical Float Data

The Biogeochemical (BGC) float data that was used in this study came from float 5905108 released by the National Oceanic and Atmospheric Administration's (NOAA) Atlantic Oceanographic and Meteorological Laboratory (AOML). This

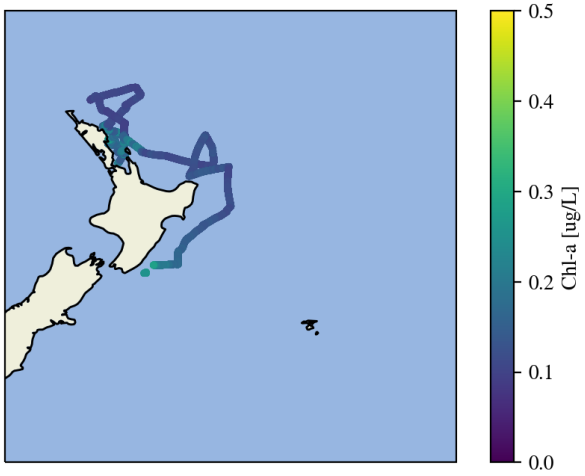

Fig. 5. Locations and calibrated values of flow-through data points from the *Seamans* cruise track displayed on map

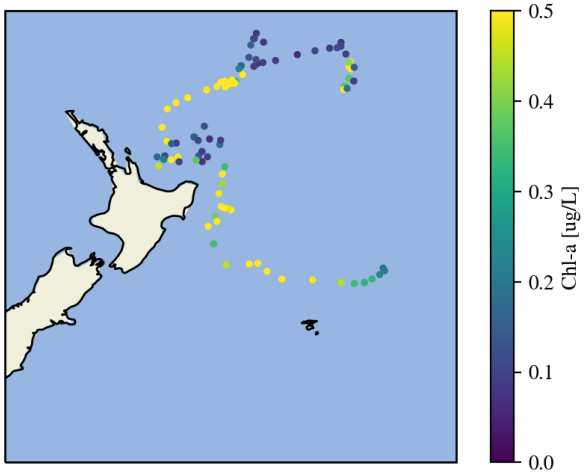

Fig. 6. Computed chlorophyll *a* values from surface BGC Argo data visualized on a map

float was selected because it was the only float equipped with a chlorophyll *a* fluorometer that traveled within the area relevant to this study based on the floats visible on the BGC Argo website (http://www.oao.obs-vlfr.fr/mapsg/en/). The raw data for this float was obtained from the US-GODAE GDAC FTP site (ftp://usgodae.org/pub/outgoing/argo/dac/aoml/5905108/) and spans a time period between July 29th, 2017 to February 3rd, 2020.

The BGC float data in its raw form is difficult to compare to satellite data since it is three-dimensional, contrary to the two-dimensional nature of the satellite data. To reduce the dimensionality of the BGC data, a chlorophyll value was computed for each station by integrating the chlorophyll measurements from the surface to the approximate mixed layer depth (20 meters) using Ocean Data View, then normalizing the data in Python. Since this data is recorded in units of $\mu g/L$, no additional calibration or unit conversion was necessary. The results from this computation for each station can be viewed in Figure 6.

E. Remote Sensing Data

The remote sensing data used in this study came from the VIIRS-SNPP dataset available from NASA's OceanColor Web (https://oceancolor.gsfc.nasa.gov/l3/order/). The product data used was from the default chlorophyll algorithm applied over an 8-day period with a 4 kilometer resolution. Data used in this paper ranged from July 4th, 2017 (right before the first station of BGC Argo float 5905108) to March 12th, 2020 (to cover the last flow-through data point). Since this data is recorded in units of $\mu g/L$, no additional calibration or unit conversion was necessary. Sample visualizations of this data can be viewed in Figure 7.

F. Chlorophyll a Measurement Comparison

In order to effectively compare the flow-through and BGC Argo chlorophyll *a* data with the remote sensing data, the

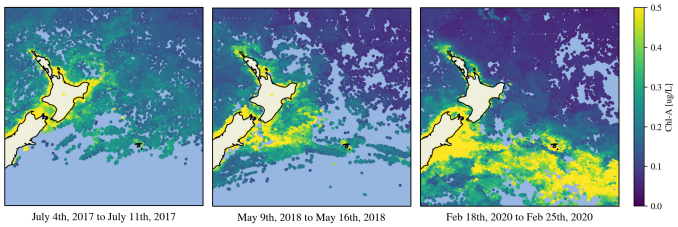

Fig. 7. Chlorophyll *a* values from the VIIRS-SNPP dataset during three different time periods. Points were downsampled by a factor of 10 to create this visualization.

data needs to be temporally and spatially synced as much as possible. To achieve this, a lookup table containing satellite data was established. For each data point in the flow-through and BGC Argo datasets, the chlorophyll *a* value for the nearest point spatially in the satellite data from the appropriate time period was recorded.

The Python code used to create the figures in this section can be viewed online at https://github.com/AmyPhung/chl-a-comparison/

III. Results

Comparisons between BGC Argo and satellite chlorophyll *a* data are presented in Figure 8.

As evident by Figure 8, there is a distinct difference in the relationship between the BGC Argo and satellite data for lower and higher chlorophyll *a* values. When the points are directly compared to each other, two distinct clusters are visually apparent due to this difference as illustrated by Figure 9. To compute these clusters mathematically, a Gaussian mixture model is used to label each point. [3] A best-fit TLS regression line is then applied to quantify the relationship between the

[3]A Gaussian mixture model was chosen over other clustering methods due to its ability to cluster "stretched-out" data. A good explanation of this can be found here: https://jakevdp.github.io/PythonDataScienceHandbook/05.12-gaussian-mixtures.html

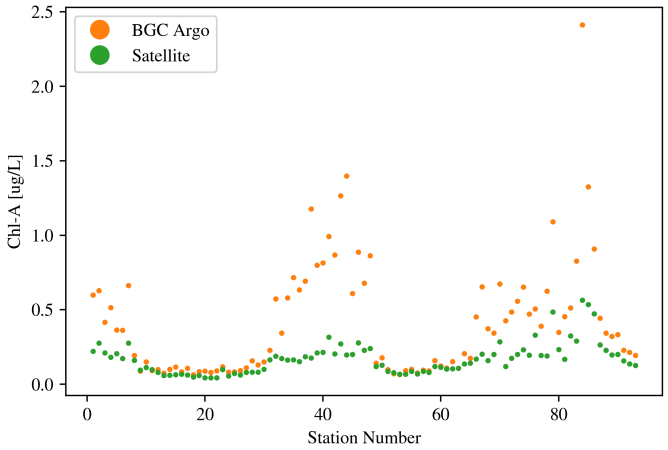

Fig. 8. Chlorophyll *a* data comparison between BGC Argo and remote sensing collection methods by station.

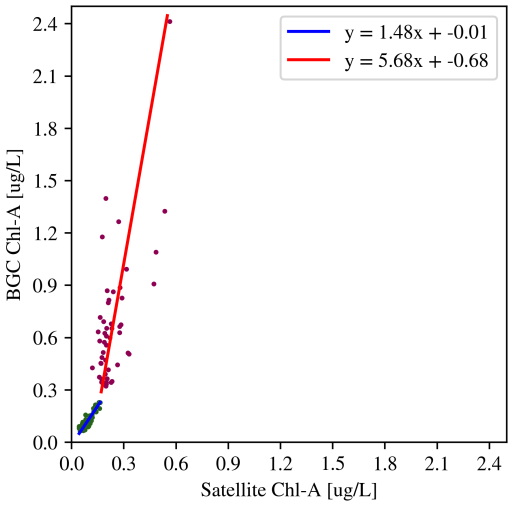

Fig. 9. Chlorophyll *a* data comparison between BGC Argo and remote sensing collection methods directly. Points are colored based on results from using a Gaussian mixture model for clustering to distinguish between high and low-concentration points. Best-fit TLS regression lines computed for each cluster are also displayed.

two datasets for each point the within each cluster. The results from this analysis are displayed in Figure 9.

To quantify the agreement between the two datasets, the percent difference between the BGC Argo and satellite datasets for each point was computed using the following equation

$$(\%D) = \frac{n_1 - n_2}{\frac{n_1+n_2}{2}} \times 100 \quad (1)$$

where n_1 is the BGC Argo value and n_2 is the satellite value.[4]

[4]This equation differs slightly from the typical percent difference formula since there is no absolute value around the difference between n_1 and n_2. By keeping n_2 as the satellite value, the resulting sign of the percent difference indicates whether n_1 is higher or lower than the value measured by the satellite

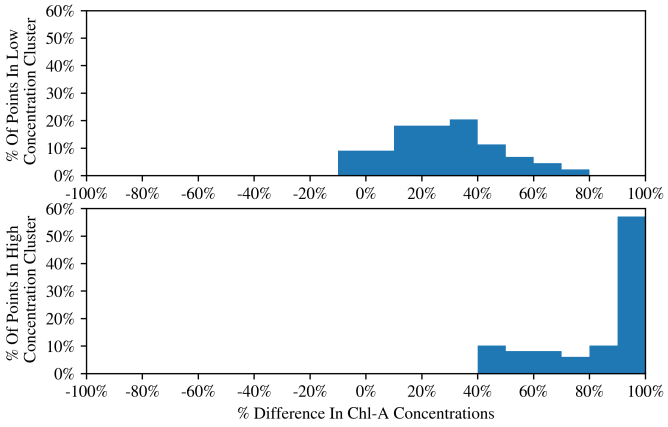

Fig. 10. Histogram of points grouped based on the percent difference between the satellite and BGC Argo data with a bin size of 10%. Points greater than 100% or less than −100% off were grouped with the bins on the edge.

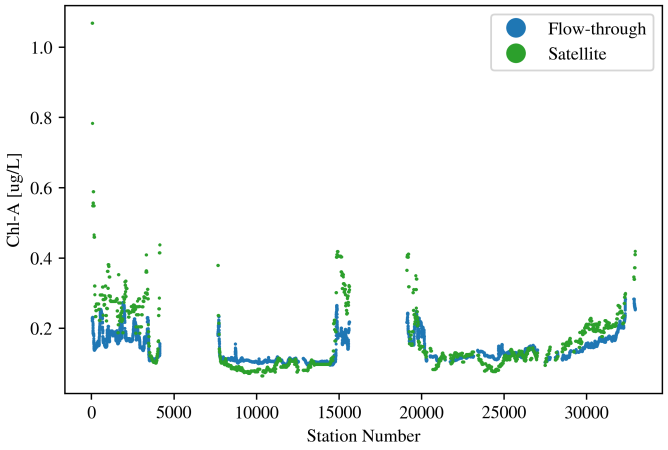

Fig. 11. Chlorophyll *a* data comparison between flow-through and remote sensing collection methods by station.

A histogram of the percent differences in the data for each of the two clusters can be found in Figure 10.

The same analysis can also be used to compare the flow-through and satellite chlorophyll *a* data. A comparison of the values by station can be viewed in Figure 11. For data points without a corresponding satellite measurement (due to cloud cover or other reasons), the measurement was dropped.

Similar to the BGC Argo dataset, there is a distinct difference in the relationship between the flow-through and satellite data for higher chlorophyll *a* concentrations. Because of this, we can once again use a Gaussian mixture model and two regression lines to characterize the relationship between these datasets. The results are illustrated in Figure 12.

A histogram displaying the percent differences in the data for each of the two clusters can be found in Figure 13

The average percent difference for the two datasets are presented in Table I.

The Python code used to create the figures in this section can be viewed and online at https://github.com/AmyPhung/chl-

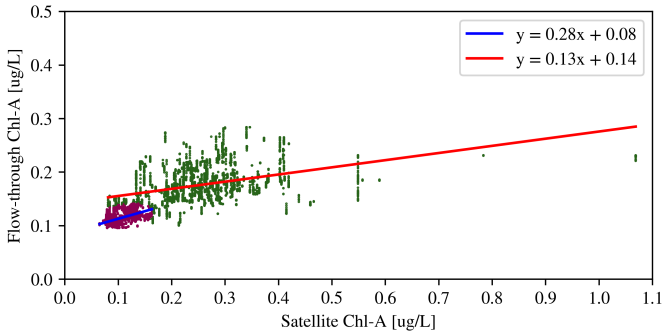

Fig. 12. Chlorophyll *a* data comparison between flow-through and remote sensing collection methods directly. Points are colored based on results from using a Gaussian mixture model for clustering to distinguish between high and low-concentration points. Best-fit TLS regression lines for each cluster are also displayed

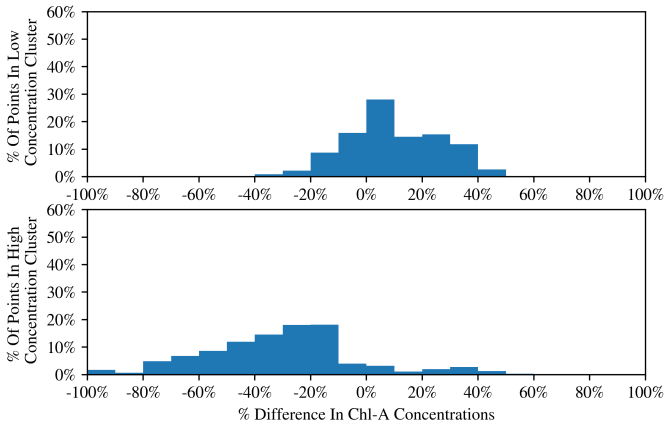

Fig. 13. Histogram of points grouped based on the percent difference between the satellite and flow-through data with a bin size of 10%. Points greater or less than 100% off were grouped with the bins on the edge.

a-comparison/.

IV. Discussion

Overall, there was generally good agreement between data points of different sources in relatively low chlorophyll *a* concentrations, but data collected in areas with high chlorophyll *a* concentrations differed significantly. It's worth noting that the edge between the high and low concentration clusters occurred at approximately 0.2 $\mu g/L$ in the BGC Argo dataset and at approximately 0.15 $\mu g/L$ in the flow-through dataset. This observation may be an artifact of how the chlorophyll *a* concentrations are computed with the remote sensing data. The default chlorophyll *a* algorithm used to compute the data used in this paper employs the standard OC3/OC4 (OCx) band ratio algorithm merged with the color index (CI) of Hu et al. (2012). The current implementation transitions between CI and OCx at $0.15 < \text{CI} < 0.2$ mg/m^3 (https://oceancolor.gsfc.nasa.gov/data/viirs-snpp/), which is interesting because that's precisely where the trends between the datasets change.

TABLE I
Average percent differences for different sub-sets of data

Dataset	% Difference
Flow-through/Satellite (Low concentrations)	10.10%
Flow-through/Satellite (High concentrations)	−30.60%
Flow-through/Satellite (Overall)	−6.06%
BGC Argo/Satellite (Low concentrations)	27.87%
BGC Argo/Satellite (High concentrations)	89.95%
BGC Argo/Satellite (Overall)	60.58%

A. Comparisons at Low Concentrations

For both the flow-through and BGC Argo datasets, the agreement with reported chlorophyll *a* levels from the satellite is much better and more consistent in areas with lower concentrations. The low-concentration histogram distribution for both datasets look relatively similar to each other, but the BGC Argo dataset is centered at 30% while the flow-through dataset is centered at 10%.

At low concentrations, there is a remarkably strong linear relationship between the BGC Argo and satellite data, as evident by the blue best fit line in Figure 9. Although the average percent difference between the flow-through and satellite data at low concentrations (10.1%) is lower than that of the average difference between the BGC Argo and satellite data (27.87%), the flow-through's linear relationship with the satellite data is not as strong. This is evident by the variability in the data around the blue best-fit line in Figure 12.

B. Comparisons at High Concentrations

At high concentrations, both datasets don't match up with the satellite data particularly well. The BGC Argo data consistently reports higher values than the satellite data reports, with the average percent difference between the data at 89.61% as reported by Table I. However, there is still a good linear relationship between the datasets, as illustrated by the best-fit line in Figure 9. Meanwhile, the flow-through data consistently reports lower values than the satellite does at high concentrations, with the average percent difference between the data at -29.47% as reported by Table I. Unlike the BGC Argo dataset, however, there is not a great linear relationship between the flow-through and satellite data at high concentrations as evident by Figure 12.

In the first few hours of the flow-through dataset, there is a notable spike in the satellite chlorophyll *a* values as evident in Figures 11 and 12 as the ship passed through the Hauraki Gulf. A multi-year study done in 2013 by Pinkerton et al. [19] that focused on comparing in-situ measurements with the MODIS-Aqua (the predecessor to VIIRS) satellite data found that "long-term median concentrations in inshore regions are higher in the satellite data set by about a factor of 2." Similar to the observations in that study, the significant discrepancy between our observed flow-through and satellite measurements in that region may be partly due to the flow-through data missing brief productivity events that the satellite would've incorporated into its measurements. However, more data from

this particular region over a wider timescale is needed to make more conclusive claims about VIIRS data in this region.

C. BGC Data Quality Over Time

Although previous studies have documented sensor drift in some BGC Argo floats over time, it's worth noting that there was no significant observable drift in the float used in this study past what has already been accounted for. At high concentrations, there is a notable divergence in the satellite and BGC Argo datasets as Figure 8 illustrates, but this trend does not appear to change over time. The low-concentration best-fit line computed for the data in Figure 9 also features a y-intercept value rather close to 0, which suggests that there is not an offset caused by sensor drift in the data.

V. Conclusion

Across the flow-through, BGC Argo, and VIIRS-SNPP datasets, there was generally good agreement between reported chlorophyll a values in lower concentrations (below approximately 0.15-0.2 $\mu g/L$), but in higher concentrations the data between each of the sources differed significantly. In low-concentration areas, the flow-through and BGC Argo datasets both generally reported values a higher than values reported by the satellite, with average percent differences being 10.4% and 27.86% respectively. The BGC Argo dataset had good linear relationships with the satellite data in both low and high concentrations, though it's worth noting that the relationship was different for each concentration level. While the flow-through dataset generally had better agreement with the satellite data than the BGC Argo dataset did, it had poorer linear relationships with the satellite data at both low and high concentrations. At high-concentrations, the BGC Argo data tended to report values significantly higher than the recorded satellite values while the flow-through tended to report significantly lower values.

To continue this study, incorporating data from BGC floats in a wider region and adding in data from floats as they're introduced into the area would allow for a greater understanding of the variations between different floats and provide more data points to work with. Incorporating flow-through datasets from previous cruise tracks in the same region to expand the distribution in time for the flow-through data would also be a good next step.

VI. Acknowledgements

I would like to thank Professor Jan Witting for his invaluable inputs and guidance on the research direction and analysis. Flow-through data was collected onboard the SSV Robert C. Seamans, operated by Sea Education Association, with support from SEA faculty, staff, and SEA Semester students.

References

[1] M. J. Behrenfeld and P. G. Falkowski, "Photosynthetic rates derived from satellite-based chlorophyll concentration," *Limnology and Oceanography*, vol. 42, no. 1, pp. 1–20, 1997.

[2] K. Carder, F. Chen, J. Cannizzaro, J. Campbell, and B. Mitchell, "Performance of the modis semi-analytical ocean color algorithm for chlorophyll-a," *Advances in Space Research*, vol. 33, no. 7, pp. 1152 – 1159, 2004, climate Change Processes in the Stratosphere, Earth-Atmosphere-Ocean Systems, and Oceanographic Processes from Satellite Data.

[3] C. Hu and J. Campbell, *Oceanic Chlorophyll-a Content*. Berlin, Heidelberg: Springer Berlin Heidelberg, 2014, pp. 171–203.

[4] R. C. Smith, K. S. Baker, and D. Phillip, "Fluorometric techniques for the measurement of oceanic chlorophyll in the support of remote sensing," 1981.

[5] C. Hu, Z. Lee, and B. Franz, "Chlorophyll-a algorithms for oligotrophic oceans: A novel approach based on three-band reflectance difference," *Journal of Geophysical Research: Oceans*, vol. 117, no. C1, 2012.

[6] M. Kahru, "Ocean productivity from space: Commentary," *Global Biogeochemical Cycles*, vol. 31, no. 1, pp. 214–216, 2017.

[7] Z. Lee, A. Weidemann, J. Kindle, R. Arnone, K. L. Carder, and C. Davis, "Euphotic zone depth: Its derivation and implication to ocean-color remote sensing," *Journal of Geophysical Research: Oceans*, vol. 112, no. C3, 2007.

[8] S. M. Glenn, T. D. Dickey, B. Parker, and W. Boicourt, "Long-term real-time coastal ocean observation networks," *Oceanography*, vol. 13, no. 1, pp. 24–34, 2000.

[9] H. C. Bittig, T. L. Maurer, J. N. Plant, C. Schmechtig, A. P. S. Wong, H. Claustre, T. W. Trull, T. V. S. Udaya Bhaskar, E. Boss, G. Dall'Olmo, E. Organelli, A. Poteau, K. S. Johnson, C. Hanstein, E. Leymarie, S. Le Reste, S. C. Riser, A. R. Rupan, V. Taillandier, V. Thierry, and X. Xing, "A bgc-argo guide: Planning, deployment, data handling and usage," *Frontiers in Marine Science*, vol. 6, p. 502, 2019.

[10] A. Earp, C. E. Hanson, P. J. Ralph, V. E. Brando, S. Allen, M. Baird, L. Clementson, P. Daniel, A. G. Dekker, P. R. Fearns, J. Parslow, P. G. Strutton, P. A. Thompson, M. Underwood, S. Weeks, and M. A. Doblin, "Review of fluorescent standards for calibration of in situ fluorometers: Recommendations applied in coastal and ocean observing programs," *Opt. Express*, vol. 19, no. 27, pp. 26 768–26 782, Dec ts.

[11] G. C. Chang and R. W. Gould, "Comparisons of optical properties of the coastal ocean derived from satellite ocean color and in situ measurements," *Opt. Express*, vol. 14, no. 22, pp. 10 149–10 163, Oct 2006.

[12] M. Szeto, P. J. Werdell, T. S. Moore, and J. W. Campbell, "Are the world's oceans optically different?" *Journal of Geophysical Research: Oceans*, vol. 116, no. C7, 2011.

[13] C. Guinet, X. Xing, E. Walker, P. Monestiez, S. Marchand, B. Picard, T. Jaud, M. Authier, C. Cotté, A. C. Dragon, E. Diamond, D. Antoine, P. Lovell, S. Blain, F. D'Ortenzio, and H. Claustre, "Calibration procedures and first dataset of southern ocean chlorophyll a profiles collected by elephant seals equipped with a newly developed ctd-fluorescence tags," *Earth System Science Data*, vol. 5, no. 1, pp. 15–29, 2013.

[14] O. A. Bukin, A. N. Pavlov, M. S. Permyakov, A. Y. Major, O. G. Konstantinov, A. V. Maleenok, and S. A. Ogay, "Continuous measurements of chlorophyll-a concentration in the pacific ocean by shipborne laser fluorometer and radiometer: Comparison with seawifs data," *International Journal of Remote Sensing*, vol. 22, no. 2-3, pp. 415–427, 2001.

[15] K. S. Johnson, J. N. Plant, L. J. Coletti, H. W. Jannasch, C. M. Sakamoto, S. C. Riser, D. D. Swift, N. L. Williams, E. Boss, N. Haëntjens, L. D. Talley, and J. L. Sarmiento, "Biogeochemical sensor performance in the soccom profiling float array," *Journal of Geophysical Research: Oceans*, vol. 122, no. 8, pp. 6416–6436, 2017.

[16] C. Roesler, J. Uitz, H. Claustre, E. Boss, X. Xing, E. Organelli, N. Briggs, A. Bricaud, C. Schmechtig, A. Poteau, F. D'Ortenzio, J. Ras, S. Drapeau, N. Haëntjens, and M. Barbieux, "Recommendations for obtaining unbiased chlorophyll estimates from in situ chlorophyll fluorometers: A global analysis of wet labs eco sensors," *Limnology and Oceanography: Methods*, vol. 15, no. 6, pp. 572–585, 2017.

[17] P. Boggs, "Orthogonal distance regression," 1989.

[18] F. Pedregosa, G. Varoquaux, A. Gramfort, V. Michel, B. Thirion, O. Grisel, M. Blondel, P. Prettenhofer, R. Weiss, V. Dubourg, J. Vanderplas, A. Passos, D. Cournapeau, M. Brucher, M. Perrot, and E. Duchesnay, "Scikit-learn: Machine learning in Python," *Journal of Machine Learning Research*, vol. 12, pp. 2825–2830, 2011.

[19] M. Pinkerton, S. Wood, J. Zeldis, and M. Gall, "Satellite ocean-colour remote sensing of the hauraki gulf marine park," Waikato Regional Council, Tech. Rep., 2013.